# Characterization of the microstructure of dairy systems using automated image analysis

Juliana V.C. Silva, David Legland, Chantal Cauty, Irina Kolotuev, Juliane Floury

HAL Id: hal-01130408

https://univ-rennes.hal.science/hal-01130408

Submitted on 11 Mar 2015

Concentrated
milk suspensions

High pressure freezing and
Freeze-substitution for **TEM**

Concentrated
milk gels

**Image analysis**

**Determination of
microstructural parameters**

Inter-particle
distance

Particle size

Inter-particle
aggregate
distance

Particle
aggregate
size

$$\text{Boundary length per unit area} = \frac{\text{boundary length}}{\text{total area}}$$

$$\text{Area fraction} = \frac{\text{color area}}{\text{total area}} \qquad \text{Porosity} = \frac{\text{white area}}{\text{total area}}$$

**Structure-property**
relationships
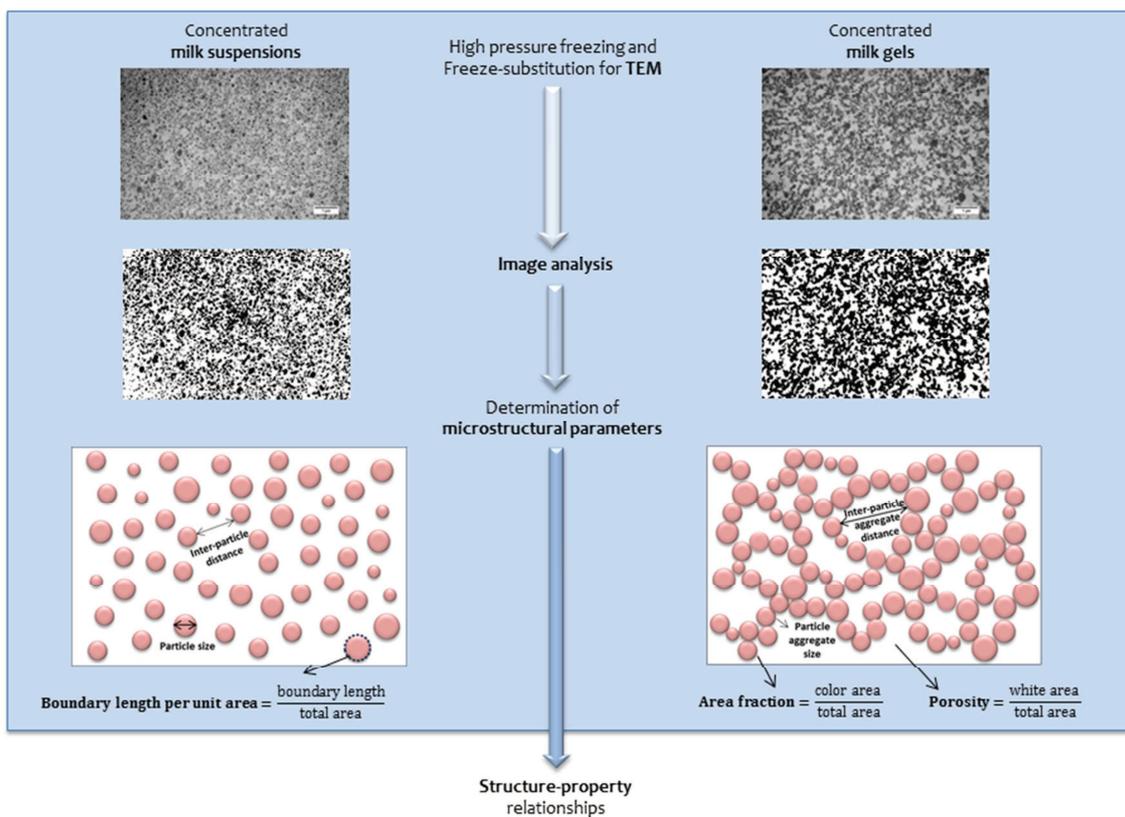
1 **Characterization of the microstructure of dairy systems using automated image analysis**

2

3 **Juliana V. C. Silva[a], David Legland[b,c,d,e], Chantal Cauty[a], Irina Kolotuev[f,g], Juliane**

4 **Floury[a,h,*]**

5 [a]INRA, UMR1253 Science and Technology of Milk and Eggs, F-35042 Rennes, France

6 [b]INRA, UMR782 Food Process Engineering and Microbiology, F-78850 Thiverval-Grignon,

7 France

8 [c]AgroParisTech, UMR782 Food Process Engineering and Microbiology, F-78850 Thiverval-

9 Grignon, France

10 [d]INRA, UMR1318 Institut Jean-Pierre Bourgin, F-78026 Versailles, France

11 [e]AgroParisTech, Institut Jean-Pierre Bourgin, F-78026 Versailles, France

12 [f]MRic-TEM, UMS3480 Microscopy Rennes Imaging Center, F-35043 Rennes, France

13 [g]IGDR, UMR6290 University of Rennes 1, 2, F-35043 Rennes, France

14 [h]Agrocampus Ouest, UMR1253 Science and Technology of Milk and Eggs, F-35042 Rennes,

15 France

16

17 [1]Corresponding author: Juliane Floury

18 Telephone number: +33 (0)2 23 48 54 52; Fax number: +33 (0)2 23 48 55 78

19 E-mail: juliane.floury@agrocampus-ouest.fr

20

21

22

23

24

25

26

**ABSTRACT**

A sound understanding of the microstructure of dairy products is of great importance in order to predict and control their properties and final quality. The aim of this study was to develop an automated image analysis procedure to characterize the microstructure of different dairy systems. A high pressure freezing coupled with freeze-substitution (HPF-FS) protocol was applied prior to transmission electron microscopy (TEM) in order to minimize any modification of the microstructure of the dairy systems investigated. The developed image analysis procedure was first validated on synthetic images of suspensions, and then on two types of concentrated milk suspensions. Microstructural data relating to casein micelles in milk suspensions were taken from the literature. The established procedure was then applied to the two corresponding rennet-induced milk gels, prepared from the same milk concentrates used for suspensions preparation. The automated image analysis procedure allowed the reliable estimation of several characteristic microstructural parameters including area fraction, porosity, boundary length per unit area, particle aggregate size, inter-particle aggregate distance and tortuosity. The relative ease of estimating these microstructural parameters from the automated image analysis method could make it useful for routine measurements of milk gels. Moreover, the method enabled a useful discrimination between two different types of milk gels. This novel approach can contribute to a better understanding of the effects of processing on the structure-property relationships in dairy products, and may be applied to other food systems.

52 **1. Introduction**

53

54    The microstructure is one of the major determining factors of flavor, physicochemical

55  and of the functional properties of dairy products. Thus understanding the microstructure of

56  dairy products during their manufacture and subsequent storage is of great importance in

57  order to predict and control their properties and final quality (Gunasekaran & Ding, 1999; El-

58  Bakry & Sheehan, 2014).

59    Dairy products are principally based on caseins, which make up 80% of the protein in

60  milk. Around 95% of the caseins in milk exist as large colloidal particles between 50 and 600

61  nm in diameter (mean ~120 nm), which are known as "casein micelles" (Fox & Brodkorb,

62  2008). The microstructure of dairy products depends principally on the organization of these

63  casein micelles that can change as a function of the technological treatment applied to milk.

64  For instance, casein micelles are easily destabilized by adding rennet to milk to form a rennet-

65  induced gel, the basis of cheese making (Lucey, 2002; Dalgleish & Corredig, 2012). In

66  contrast to milk, where caseins are present in suspension, milk gels form a continuous three

67  dimensional network whose properties greatly depend on the microstructure.

68    The microstructure of dairy products is commonly investigated using instrumental

69  techniques such as light or electron microscopy techniques. Light microscopy, such as

70  Confocal Laser Scanning Microscopy (CLSM), allows the observation of dairy products with

71  a minimum of sample preparation and with a resolution up to 0.25 microns (Fenoul, Le

72  Denmat, Hamdi, Cuvelier, & Michon, 2008; Morand, Guyomarc'h, Legland, & Famelart,

73  2012; Ercili-Cura et al., 2013). By using this technique, it may be possible to distinguish the

74  structure of the milk gel, but not the fine organisation of casein micelles that form its

75  microstructure. Electron microscopy provides a resolution at a nanometer scale, making it

76  possible to observe the organization of the gel protein network itself. Scanning Electron

3

77 Microscopy (SEM) has already been used for investigating the microstructure of a variety of

78 dairy products (Marchesseau, Gastaldi, Lagaude, & Cuq, 1997; McMahon, Fife, & Oberg,

79 1999; Fallico et al., 2006; Le Feunteun & Mariette, 2007; 2008). However, SEM provides

80 only a topographical view of the sample surface, making it difficult to quantify properties

81 from the observed images. On the other hand, Transmission Electron Microscopy (TEM)

82 provides observation of a slice of the sample, making it possible to investigate its internal

83 structure. This can provide a basis for the quantitative description of the sample

84 microstructure (Reis & Malcata, 2011).

85 Conventional TEM preparation procedures include chemical fixation, dehydration and

86 embedding, which are frequently problematic in samples with high water content. Such

87 methods can introduce numerous artifacts that alter the relationships that exist between the

88 structural components (Kalab, Allan-Wojtas, & Mistry, 1995). Therefore, the use of low-

89 temperature methods, such as freeze-fracture replication (Büchheim, 1982; McMahon &

90 McManus, 1998), freeze-substitution (Goff, Verespej, & Smith, 1999; Smith, Kakuda, &

91 Goff, 2000), cryo-TEM (Waninge, Nylander, Paulsson, & Bergenstahl, 2003; 2004) and high

92 pressure freezing coupled with freeze-substitution methods (Ramasubramanian, Webb,

93 D'Arcy, & Deeth, 2013) are preferable in order to preserve the original structure of the dairy

94 sample ahead of the conventional TEM.

95 Nowadays, qualitative interpretations of micrographs are often no longer enough.

96 Image analysis is necessary to also provide quantitative data for the analysis and design of

97 food microstructure (Aguilera, Stanley, & Baker, 2000). Such image analysis has been

98 recently introduced into dairy research for a wide range of applications (Wium, Pedersen, &

99 Qvist, 2003; Impoco, Carrato, Caccamo, & Tuminello, 2006; Rovira, Lopez, Ferrandini, &

100 Laencina, 2011; Geng, van den Berg, Bager, & Ipsen, 2011; Ong, Dagastine, Kentish, & Gras,

101 2011; 2012; 2013).

4

102       Micrograph images of dairy samples can be quantified through the morphometry of

103    individual objects or particles (Gunasekaran & Ding, 1999; Rovira et al., 2011; Impoco, Fucà,

104    Pasta, Caccamo, & Licitra, 2012; Fucà, Pasta, Impoco, Caccamo, & Licitra, 2013). When a

105    protein network cannot be easily segmented, gray level texture analysis can be used to discern

106    the variations of gray levels from confocal images (Fenoul et al., 2008; Morand et al., 2012;

107    Ercili-Cura et al., 2013). An alternative to particle-based image analysis and image texture

108    analysis is the characterization of protein network as a binary microstructure. This method

109    consists of quantifying geometrical properties of a structure that cannot be described by a set

110    of individual particles, but rather as a complex structure with voids and branches that is

111    observed in a representative window. While this approach is common in materials science

112    (Ohser & Mücklich, 2000) and for describing porous media (Torquato, 2002), to the authors'

113    knowledge no attempt have been made to quantify the microstructure of dairy products.

114       The aim of this work was thus to develop an automated image analysis procedure to

115    characterize the microstructure of dairy systems. The proposed procedure comprised the

116    automated segmentation of the protein network from TEM micrographs, and the subsequent

117    computation of microstructural parameters by assimilating the protein network to a porous

118    media. The high pressure freezing and freeze-substitution (HPF-FS) protocol was used in

119    order to minimize modification of the microstructure of dairy systems during sample

120    preparation for TEM. Microstructural parameters considered in this study included global

121    morphological parameters (area fraction, porosity, boundary length per unit area), binary

122    image granulometry, that measures the typical sizes of particles (or of particle aggregates or

123    of voids), and a tortuosity parameter that describes the microstructure at a larger scale.

124    Tortuosity is a parameter mainly related to mass transfer properties and has been measured in

125    several porous media such as rocks, sediments, soil, zeolites, biological tissues, etc. (Suman &

126    Ruth, 1993; Latour, Kleinberg, Mitra, & Sotak, 1995; Zalc, Reyes, & Iglesia, 2004; Wu, van

127 Vliet, Frijlink, & van der Voort Maarschalk, 2006; Shen & Chen, 2007; Lanfrey, Kuzeljevic,

128 & Dudukovic, 2010). Some authors have also been applying the theory of porous media to

129 food systems and have been estimating tortuosity values from diffusion coefficients in food

130 media (Crossley & Aguilera, 2001; Sam Saguy, Marabi, & Wallach, 2005). The determination

131 of tortuosity directly from image analysis would therefore be of great interest for

132 understanding the diffusion phenomena in dairy products.

133     The concept of measuring the above listed parameters using image analysis was first

134 tested on a synthetic image representing a suspension of micelles as might be observed under

135 conditions similar to the present study. The image analysis method was subsequently

136 validated on two concentrated milk suspensions of similar casein concentration, but produced

137 by different methods. Microstructural data relating to casein micelles in milk suspensions

138 were taken from the literature for validation. The method was then applied to the

139 corresponding concentrated milk gels, obtained by rennet-induced coagulation of the same

140 milk concentrates used for suspensions preparation, in order to show a wider application of

141 this procedure.

142

143 **2. Material and Methods**

144

145 *2.1. Preparation of concentrated milk suspensions and gels*

146

147     Two concentrated milk suspensions and two concentrated milk gels presenting similar

148 casein composition were produced. These dairy systems were based on two different protein

149 milk concentrates produced using either Microfiltration (MF) or Ultrafiltration (UF)

150 processes.

151

152 *2.1.1. MF concentrate*

153    The aim of the membrane filtration process developed in this study was to obtain an

154 almost pure casein concentrate, dispersed in the same aqueous phase of milk, in order to

155 mimic as much as possible the protein composition of a real cheese. Skim milk (Entremont,

156 Montauban de Bretagne, France) was initially filtered to remove contaminating bacteria using

157 the microfiltration pilot equipment GP7 fitted with a 0.8 μm Sterilox GP membrane. This

158 microfiltrate was then concentrated by microfiltration using a 0.1 μm aluminum Zircone

159 membrane. This smaller pore size allowed the concentration of the casein fraction only, the

160 size of the whey proteins in milk being sufficiently small to cross the membrane. In order to

161 increase the concentration factor of the caseins, it was necessary to proceed to a diafiltration

162 step of the concentrate, using the MF permeate instead of water in order to keep the same

163 aqueous phase of milk in the final concentrate. The permeate had been previously

164 ultrafiltrated with a 5 kD membrane to remove the whey proteins. The overall filtration

165 process allowed concentrating the total proteins of milk by a factor of 4.3. Neither NaCl nor

166 cream was added, leaving a non-salty and a non-fatty MF concentrate. The composition of the

167 MF concentrate (pH 6.6) is given in Table 1.

168

169 *2.1.2. UF concentrate*

170    The UF concentrate was produced following previously described procedures (Ulve et

171 al., 2008; Silva, Peixoto, Lortal, & Floury, 2013). Unlike microfiltration, the ultrafiltration

172 process allowed the concentration of all the proteins of milk, both the caseins and the whey

173 proteins. This UF concentrate has then the same protein composition as for some commercial

174 cheeses obtained by using the MMV technology, such as Pavé d'Affinois (Maubois, Mocquot,

175 & Vassal, 1969; Maubois & Mocquot, 1971; Maubois & Mocquot, 1975). Overall, the total

176 proteins of milk were concentrated in this case by a factor of 5. Once again, neither NaCl nor

177 cream was added, leaving a non-salty and a non-fatty UF concentrate. The composition of the

178 UF concentrate (pH 6.6) is given in Table 1.

179 The MF concentrate was used without further preparation whereas the UF concentrate

180 was heated at 93°C for 15 min (Aly et al., 2011) and then cooled using melting ice for 3 min.

181 Sodium azide was added to both the MF and heat-treated UF concentrates at a final

182 concentration of 0.05% (wt/wt) in order to prevent microorganism growth. About 1 mL of the

183 MF concentrate or of the heat-treated UF concentrate were poured into 2 mL Eppendorf tubes

184 and then incubated at 30°C for 1 h and then held at 19°C for 2 h to obtain the MF-suspension

185 or the UF-suspension, respectively. Both suspensions were passively aspired by using

186 cellulose microcapillary tubes with a 200 µm inner diameter ahead of further preparation for

187 TEM.

188 The concentrated milk gels were produced from the same concentrates (i.e.; MF or

189 heat-treated UF concentrates). In this case, after adding sodium azide to the concentrates

190 (0.05% wt/wt), the coagulant agent Maxiren 180 (DSM Food Specialties, Seclin, France) was

191 added giving a final concentration of 0.03% (v/v). After homogenization, 600 µL of each

192 mixture (MF or heat-treated UF concentrate + coagulant agent) was slowly poured into mini-

193 gel cassette® systems (IFR Norwich, U.K.), containing flat gold-plated specimen carriers (0.5

194 mm thick, 1.5 mm in diameter, 200 µm deep; Leica Cat #16706898). The gel cassettes®

195 systems were incubated at 30°C for 1 h to enable coagulation and then at 19°C for 2 h to

196 obtain the final gels based on each concentrate.

197

198 *2.2. Transmission electron microscopy*

199

200 The prepared concentrated milk suspensions and gels were frozen using a Leica EM

201 PACT2 high-pressure freezer (Leica Microsystems, Vienna, Austria). The sample carriers,

202 cellulose microcapillary tubes or flat gold-plated specimen carriers, were pre-coated with 1%

203 phosphatidylcholine (Sigma-Aldrich Ltd.) diluted in chloroform to avoid sample sticking. No

204 cryo-protecting agent was added to the samples. For the freeze-substitution step, Leica EM

205 AFS2 freeze substitution machine (Leica Microsystems, Vienna, Austria) was used. The

206 frozen samples were transferred in liquid nitrogen to a processing container equipped with a

207 flat spacer (Leica Microsystems, Vienna, Austria). The frozen samples were freeze-

208 substituted in 2% osmium tetroxide diluted in anhydrous acetone. After an initial incubation

209 of 8h at -90°C the temperature was gradually (5°C/hour) raised to -30°C and samples were

210 then left for another 8h at this temperature.  The solvent-fixative solution was replaced with

211 pre-chilled mix of ethanol 3:1 resin (epon-araldite mix; Sigma-Aldrich Ltd). The temperature

212 was then gradually brought up to room temperature and further ethanol:resin substitutions

213 were done following the resin manufacturer instructions. Thin sections (90 nm) of embedded

214 samples were cut with a diamond knife using a Reichert ultramicrotome. The sections were

215 contrasted with 4% aqueous solution of uranyl acetate and observed using a JEM-1400

216 Transmission Electron Microscope (JEOL Ltd., Tokyo, Japan) operated at 120 kV

217 accelerating voltage. Digital images were acquired using the Gatan SC1000 Orius® CCD

218 camera (4008 x 2672), set up with the imaging software Gatan DigitalMicrograph™ (Gatan,

219 Pleasanton, USA).

220 Several TEM micrographs were taken on different parts of two independent samples

221 of each of the four dairy systems. Ten micrograph images were chosen independently for each

222 dairy system for further image analysis.

223 The resulting images each represented an area of 9.97 x 6.64 μm and showed the

224 microstructure of the samples at a magnification of x20000. Images were saved as 32-bit

225 grayscale dm3 images of 4008 x 2670 pixels (where 1 pixel = 2.5 nm).

226

227     *2.3. Image processing of TEM micrographs*

228

229        Several image processing steps were necessary to automatically segment the TEM

230     images of the four dairy systems (concentrated milk suspensions and gels). These steps are

231     schematically set out in Fig. 1. Each image was normalized using a blank background image

232     (obtained without sample or resin) (Fig. 1B). This permitted the removal of intensity

233     variations over the image. Histogram normalization procedure was applied and the result was

234     converted to images based on 256 shades of gray (Fig. 1C). As artifacts could be detected on

235     some micrographs, they were removed by applying a "black top-hat" operation with a square

236     structuring element of 200x200 pixels (Fig. 1D). Black top-hat is a tool (taken from

237     mathematical morphology) that enhances dark structures smaller than the chosen structuring

238     element while removing larger variations (Soille, 2003). A smoothing operator was then

239     applied (by computing the average of pixel values in a circular neighborhood with radius of

240     10 pixels) to remove the acquisition noise (Fig. 1E). The two phases were contrasted, with

241     images histograms showing two peaks (Fig. 1F). "Otsu automated threshold" is commonly

242     used for the segmentation of dairy product images (Ong et al., 2011; Hussain, Grandison, &

243     Bell, 2012; Impoco et al., 2006) and was used for the segmentation in the present study. Otsu

244     threshold consists in identifying the threshold value that best discriminates between the two

245     phases, by minimizing the intra-class variance while maximizing inter-class variance (Otsu,

246     1979). The segmentation procedure was validated by visual inspection of the binary images

247     superimposed on the original images.

248    *2.4. Quantification of microstructural parameters*

249

250    The values of the microstructural parameters determined in the present work may

251    depend on several factors such as sample thickness and image processing (i.e., filter choice,

252    segmentation threshold). Therefore, the proposed image analysis procedure was first validated

253    by comparing microstructural parameters of concentrated milk suspensions with those of both

254    synthetic images and data taken from the literature. Finally, the values of microstructural

255    parameters obtained for the different dairy systems in the same conditions could be compared

256    between them.

257

258    *2.4.1. Generation of synthetic images of a suspension*

259    In order to validate and help to interpret microstructural parameters, the developed

260    image analysis method was applied on synthetic images mimicking a theoretical suspension

261    of micelles. A set of non-overlapping balls was generated in a 3D cuboid with dimensions

262    5x5x2 µm. The diameter of the balls was chosen as 120 nm, corresponding to the mean

263    diameter of casein micelles (Fox & Brodkorb, 2008). In order to avoid edge effects, a margin

264    of 200 nm was applied on all sides. The number of balls was chosen to have a numerical

265    density equal to 160 micelles/µm$^3$, corresponding to an expected number of 8000 within the

266    cuboid. This value was chosen to generate an area fraction in the synthetic images similar to

267    the one observed for milk suspensions in the present study. To avoid overlap, a minimal

268    distance of 130 nm was imposed between the micelle centers. The physical cut was

269    represented by a horizontal slice with thickness 90 nm, and located in the middle of the

270    cuboid. An example of a synthetic suspension of micelles is shown on Fig. 2A. The

271    intersection of the slice with the set of balls was used to generate a planar binary image

272    representing a virtual observation of the model system. A resolution of 2.5 nm by pixel was

273  used, resulting in a 2000x2000 pixels binary image (Fig. 2B). Ten images were thus generated

274  to address the variability of measurement method. Due to the thickness of the slice, some

275  micelles seemed to overlap, seemingly forming small agglomerates. Other micelles present a

276  smaller section because they were not located within the sampled slice. Matlab software was

277  used both to simulate the 3D synthetic suspensions and to generate the corresponding binary

278  images (Mathworks, Natick, MA). The Free-D software was used to produce the sample

279  image of Fig. 2A (Andrey & Maurin (2005), http://free-d.versailles.inra.fr/html/freed.html).

280

281  *2.4.2. Global morphometry*

282      Global morphometry was used to determine three global microstructural parameters:

283  area fraction, porosity, and boundary length per unit area. If the sampling slice can be

284  assumed to have a small thickness relative to size of the structures, these parameters can be

285  directly related to 3D properties of the network by using stereological relations.

286      Area fraction was defined as the ratio between dark area (i.e.; the protein matrix) with

287  respect to the total area of the image. The dark area corresponds to the area covered by

288  particles (for suspensions) or by particle aggregates (for gels) in the micrograph cross-

289  sections. Porosity is the complementary parameter and can be defined as the division of the

290  void area by the total image area. In the binary image, porosity was calculated as white area

291  (free space, corresponding to the aqueous phase) as a percentage of the total area (Impoco et

292  al., 2006; Rovira et al., 2011).

293      The boundary length per unit area is the length of the perimeter around all the particle

294  edges or boundaries (for suspensions) or particle aggregate edges or boundaries (for gels),

295  divided by the total image area. The boundary length per unit area thus measures the quantity

296  of interface between the protein phase and the aqueous phase. For a comparable area density,

297  its value will be larger for systems with small structures and/or tortuous interfaces, and

12

298 smaller for systems with large structures and/or smooth interfaces. Boundary length was

299 estimated by using a discretized version of Crofton formula, which consists in counting the

300 number of intercepts with lines of various orientations, and normalized by the area of the

301 image (Ohser & Mücklich, 2000; Legland, Kiêu, & Devaux, 2007).

302

303 *2.4.3. Image morphological granulometry*

304 The typical size of particles (or particle aggregates) and inter-particle (or inter-particle

305 aggregate) distances were determined by applying binary image granulometry on the

306 segmented images. Binary image granulometry is based on image transformations depending

307 on the size of a mask referred to as a "structuring element". One of the basic transformations

308 (taken from mathematical morphology) is the morphological opening, which effectively

309 removes objects smaller than the structuring element (Soille, 2003). By applying openings of

310 increasing sizes to the dairy system images, the particles (or particle aggregates) are

311 progressively removed. The complementary transformation is morphological closing, which

312 effectively makes the voids smaller than the defined structuring element disappear. Following

313 the same process, applying closings of increasing size to the images leads to a progressive

314 elimination of the part of the image showing the voids in the structure. Thus, by either

315 method, a particle (or void) size distribution curve is produced.

316 The curve *V(i)* is generated by counting the number of pixels after each closing or

317 opening step. This is then normalized according to the initial and final number of pixels

318 *V(initial)* and *V(final)* and the finite difference is computed to build a granulometric curve:

319

$$g(i) = \frac{V(i) - V(i+1)}{V(initial) - V(final)} \tag{1}$$

320

321    In the current study, the largest size (diameter) of the disk structuring element was 121

322    pixels, corresponding to about 300 nm on the image. To reduce computation time, structuring

323    element diameters were considered with a step of 4 pixels. To compare granulometric curves

324    for a set of samples, each granulometric curve was summarized by computing its geometric

325    mean. The following weighted sum was used:

326

$$m = exp\left(\sum_{i=1}^{imax} g(i) * \log(t_i)\right) \tag{2}$$

327

328    where $g(i)$ is the percent of grey level variation for the step $i$, $t_i$ is the size of the structuring

329    element in μm and *imax* is the number of closing/opening steps (Legland, Devaux, Bouchet,

330    Guillon, & Lahaye, 2012). The geometric means of the granulometric curves obtained with

331    the openings procedure were interpreted as the average size of particles (for suspensions) or

332    particle aggregates (for gels). The geometric means of the granulometric curves obtained with

333    the closings procedure were interpreted as the average size of the aqueous phase between the

334    particles or particle aggregates.

335    A schematic representation of microstructural parameters determined for suspensions

336    and gels by using the image morphological granulometry method is given in Fig. 3.

337

338    *2.4.4. Tortuosity*

339    The tortuosity in every point in the aqueous phase can be defined as the ratio of the

340    shortest path (i.e.; avoiding the protein network) between two opposing borders of the image,

341    over the Euclidean distance between the same borders (Delarue & Jeulin, 2003; Wu et al.,

342    2006). An illustration of the tortuosity for a sample structure is given in Fig. 4. The 3D

343    tortuosity cannot be determined from 2D images, but 2D tortuosity can be used to

344 quantitatively compare the microstructure of different dairy systems observed under similar

345 conditions.

346      For points belonging to aqueous phases totally included in the protein network, no

347 path can be defined to image borders. Consequently, the tortuosity over an image was defined

348 as the average value measured at points for which shortest paths could be computed. As the

349 length of the shortest path is always greater than the Euclidean distance, the tortuosity is

350 always greater than or equal to one. The tortuosity value increases with the complexity of the

351 protein network separating the aqueous phase.

352      In order to assess the variability of the tortuosity measurement, each image was

353 divided into four sub-images, and tortuosity was calculated for each sub-image. For most

354 images, the tortuosity of the complete image was similar to the average value of the sub-

355 images (the difference being less than the standard deviation). However, for some images, the

356 difference was greater, due to large blocks of protein network that introduce a large variability

357 in the measurement.

358

359 *2.5. Software implementation*

360

361      Image processing and analysis was performed using Fiji-win64 processing software.

362 The quantification of morphological features required the development of specific plugins,

363 which are available on request from the authors, or from the Internet at http://www.pfl-

364 cepia.inra.fr/index.php?page=ijGranulometry_en,                http://www.pfl-

365 cepia.inra.fr/index.php?page=ijGeodesics_en,                http://www.pfl-

366 cepia.inra.fr/index.php?page=imMinkowski_en.

367

368

15

369    *2.6. Statistical Analysis*

370

371    The mean values of microstructural parameters obtained for the four different dairy

372    systems studied (MF-suspension, UF-suspension, MF-gel and UF-gel) were statistically

373    compared using R software (version R i386 3.0.2) (R Foundation for Statistical Computing,

374    Vienne, Austria). Results are presented with the mean value and the standard deviation. One-

375    way analysis of variance (ANOVA) and Tukey's paired comparison test were applied in order

376    to determine which means are significantly different from one another at the 95% family-wise

377    confidence level. The Student's test was applied in order to compare the two suspensions and

378    the two gels.

379

380    **3. Results and Discussion**

381

382    *3.1. Image processing of TEM micrographs*

383

384    Sample images of TEM acquisition obtained by using the HPF-FS protocol are

385    presented in Fig. 5, for both pairs of suspensions and gels. The dark phase corresponds to the

386    protein matrix (i.e.; particles or particle aggregates). The lighter phase corresponds to the

387    aqueous phase, formed by water, lactose, minerals and free amino acids. In all dairy systems,

388    the particles and particle aggregates were homogeneously distributed.

389    The particle aggregates observed in the gels (Fig. 5C and 5D) are larger compared to

390    the individual particles in suspensions (Fig. 5A and 5B).

391    Representative segmented TEM micrographs of the concentrated milk suspensions and

392    gels are illustrated in Fig. 6. These segmented images correspond to the TEM micrographs

393    shown in Fig. 5. The black phase of the segmented micrographs corresponds to the protein

16

394    matrix (i.e.; particles or particle aggregates), while the white phase corresponds to the

395    aqueous phase.

396

397    *3.2. Quantification of microstructural parameters*

398

399    *3.2.1. Validation of the automated image analysis procedure*

400         Microstructural parameters were measured for the two concentrated milk suspensions

401    in order to validate the image processing of TEM micrographs by comparing with values

402    taken from the literature. Obtained values were also compared to those obtained on synthetic

403    suspension images. Table 2 presents the values of the microstructural parameters obtained

404    from TEM micrographs of the milk suspensions.

405         Area fractions measured from TEM micrographs were equal to $0.34 \pm 0.02$ and $0.33 \pm$

406    $0.01$ for the MF- and UF-suspensions, respectively. Area fractions did not differ statistically

407    ($p < 0.05$) between the MF- and UF-suspensions. This fact can be explained by the same

408    casein concentration in both suspensions (130 g/kg).

409         The number of micelles in the synthetic suspension image was adjusted to obtain a

410    value of area fraction similar to that for the real suspensions. The related value for the

411    synthetic images was equal to $0.338 \pm 0.005$. The other microstructural parameters can

412    therefore be compared between synthetic and real suspensions.

413         The mean particle size obtained by granulometry on the synthetic suspension images

414    was estimated as $116.3 \pm 0.3$ nm. This is very close to the diameter of the casein micelles,

415    validating the image analysis method in this respect. Nonetheless, the measured values on the

416    synthetic suspension images were still smaller than the real diameter of casein micelles, which

417    is attributed to the presence of smaller sections of micelles.

17

418       Fig. 7 shows granulometric curves for the milk suspensions representing the particle

419    size distribution (Fig. 7A and 7B for MF- and UF-suspensions, respectively) and the

420    distribution of inter-particle distances (Fig. 7C and 7D for MF- and UF-suspensions,

421    respectively). A good repeatability of the particle size distributions and of inter-particle

422    distance is noted for both MF- and UF-suspensions. The corresponding mean particle size and

423    inter-particle distance values from the geometric means are given in Table 2.

424       The mean particle size was $88 \pm 3$ nm and $99 \pm 4$ nm for the MF- and UF-suspensions.

425    At the casein concentration used (130 g/kg, corresponding to ~140 g/L for these suspensions),

426    casein micelles are fully separated from each other, i.e., below the concentration of random-

427    close packing estimated as ~178 g/L (Bouchoux, Debbou, Gésan-Guiziou, Famelart, &

428    Doublier, 2009). Casein micelles present in milk are known to have a broad size distribution

429    with diameters ranging from 50 to 500 nm, and a mean diameter of ~120 nm (Fox &

430    Brodkorb, 2008). The values obtained by image analysis fall within this range of diameters

431    found for casein micelles in unconcentrated milk, but are smaller than the indicated mean

432    diameter. Similar results were reported by Srilaorkul et al. (1991), who studied the effect of

433    skim milk ultrafiltration on particle size using conventional TEM. They measured particle size

434    by observation using a Baush and Lomb measurement magnifier, counting and classifying the

435    micelles into 10 classes, each with a width of 20 nm. They saw a decrease in mean casein

436    micelle diameter from 118 nm in normal milk to 87 nm in milk that had been concentrated

437    five times. The change in the composition of casein and minerals as a result of the

438    ultrafiltration of milk may be responsible for the change in average diameter of the casein

439    micelles.

440       The UF-suspension presented a mean particle size greater than that for the MF-

441    suspension. The larger mean particle size (of about 10 nm) for the UF-suspension may be due

442    to the association of denatured whey proteins on the surface of the micelles due to the heat

443  treatment applied to the UF concentrate (Jeurnink & de Kruif, 1993; Anema & Li, 2003; Nair,

444  Dalgleish, & Corredig, 2013). Anema & Li (2003) demonstrated that the diameter of casein

445  micelles in heated reconstituted skim milk increased by 19 nm as a consequence of heat

446  treatments. For the concentrated milk studied in the same work, prepared by subjecting milk

447  to a combination of ultrafiltration and microfiltration techniques, an overall increase of 5 nm

448  was observed when samples at pH 6.55 were heated for 45 min at 90°C. These values are

449  comparable to the increase of about 10 nm of mean particle size found in the current study for

450  the (heat-treated) UF-suspension.

451      The mean inter-particle distance obtained from the image analysis was 123 ± 5 nm and

452  132 ± 2 nm for the MF- and UF-suspensions, respectively. These values are smaller than

453  those predicted from the synthetic suspension (153 ± 3 nm). This may be explained by the

454  differences in the diameter distribution: as real suspensions contain a larger number of small

455  micelles the mean free distance will be less. The mean free distance between casein micelles

456  in unconcentrated milk is reported as around 240 nm (Fox & Brodkorb, 2008). As expected,

457  the mean inter-particle distances between the casein micelles would be smaller in the

458  concentrated milk suspensions than in milk (25 g/L) due to the higher casein concentration

459  (130 g/kg, i.e. around 140 g/L) as a result of the membrane technology (microfiltration or

460  ultrafiltration processes) applied. It is known that when the concentration of total solids in

461  skim milk increases (e.g. during ultrafiltration), the distance between the casein micelles

462  decreases due to the increased volume fraction (Karlsson, Ipsen, Schrader, & Ardö, 2005).

463      The images of the MF- and UF-suspensions presented similar area fraction values

464  whereas the particle size and inter-particle distance values were statistically different. The

465  mean inter-particle distance was greater for the UF-suspension (when compared with the MF-

466  suspension) that counteracted, to some extent, the effect of the larger mean particle size.

467    The MF-suspension images presented a boundary length per unit area of 13.3 ± 0.5

468    $\mu m/\mu m^2$, and the UF-suspension a value of 12.1 ± 0.2 $\mu m/\mu m^2$. This parameter is a measure of

469    the quantity of interface between the protein phase (black phase) and the aqueous phase

470    (white phase). For comparison, the values measured for the synthetic suspension images were

471    11.5 ± 0.2 $\mu m/\mu m^2$. This may be explained by the fact that synthetic suspensions are more

472    regular than real ones. The value was significantly larger for the MF-suspension than for the

473    UF-suspension. This result may have been expected because a suspension with small particles

474    (MF-suspension) will have a greater interface (between the particles and the aqueous phase)

475    and thus a larger boundary length per unit area value. As both suspensions have the same area

476    fraction, the observed difference depends on the regularity of the interface. Assuming a

477    suspension of spherical particles, an interpretation is that the MF-suspension is composed of

478    smaller particles compared with the UF-suspension.

479    The tortuosity was 1.08 ± 0.01 for the MF-suspension and 1.06 ± 0.01 for the UF-

480    suspension. These values were not significantly different ($p < 0.05$) but they were a little bit

481    larger than that for the synthetic suspensions (1.043 ± 0.001). It can be observed that

482    tortuosity value increases when mean distance between micelles decreases, and when

483    boundary length per unit area increases.

484    Overall, the microstructural parameter values predicted for concentrated milk

485    suspensions by the image analysis procedure were in agreement with literature findings and

486    also with results obtained for a synthetic suspension. This fact allowed us to validate the

487    image processing of TEM micrographs.

488

489

490

491

20

492    *3.2.2. Application of the automated image analysis procedure to milk gels*

493    The image analysis procedure validated previously for the two types of concentrated

494    milk suspensions was then applied to their corresponding gels, which had been obtained by

495    rennet-induced coagulation, in order to determine their microstructural parameters.

496    The microstructure of milk gels is more complex than that for suspensions and

497    depends on several factors such as the type of coagulation and the treatment applied to the

498    milk concentrate prior to the coagulation step. It is well known that the addition of chymosin

499    cleaves a specific bond of the κ-casein on the surface of the micelles. This reduces the steric

500    and electrostatic repulsion between the micelles, and the destabilized micelles thus begin to

501    aggregate to form the gel (Mellema, Heesakkers, van Opheusden, & van Vliet, 2000).

502    Table 3 sets out the values for the microstructural parameters obtained from the TEM

503    images of MF- and UF-gels.

504    The mean area fractions were 0.49 ± 0.03 and 0.50 ± 0.02 for MF- and UF-gels,

505    respectively, which were significantly ($p < 0.05$) larger than the values obtained for the

506    related suspensions (0.34 ± 0.02 and 0.33 ± 0.01 for MF- and UF-suspensions, respectively).

507    However, similar area fraction values should be expected for concentrated milk suspensions

508    and gels presenting the same casein concentration. This unexpected result may be explained

509    by the aggregation of casein micelles in the gel which could induce changes in the apparent

510    density of particles on the TEM images, due to the slice thickness of the sample.

511    Curds from heat-treated milks tend to be weak, ragged in appearance with a poor

512    matting ability and poor fusion of the gel network, giving rise to more porous matrices (Singh

513    & Waungana, 2001). However, in the present study, the UF-gel (made from heat-treated UF

514    concentrate) presented the same porosity compared with the MF-gel (about 0.50). This fact

515    can be explained by the ultrafiltration of the milk prior to coagulation in the case of the UF-

516    gel. It is known that gels formed from UF concentrates are much firmer than the

517  corresponding curds produced from unconcentrated milks at comparable levels of β-

518  lactoglobulin denaturation and association (Singh & Waungana, 2001). This result is

519  interesting because gels obtained from different technological treatments but with the same

520  casein composition have a similar porosity. Thus, heat treatment in combination with

521  concentration processes such as ultrafiltration may yield opportunities to correct curd

522  properties.

523  Fig. 8 shows granulometric curves obtained by applying the opening procedure (Fig.

524  8A and 8B for MF- and UF-gels, respectively), representing the distribution of particle

525  aggregate sizes and by the closing procedure (Fig. 8C and 8D for MF- and UF-gels,

526  respectively), representing the distribution of inter-particle aggregate distances obtained from

527  TEM micrographs. Fig. 8 demonstrates the good repeatability of the distribution of particle

528  aggregate size and inter-particle aggregate distance values obtained from different TEM

529  micrographs of the MF- and UF-gels. Values for these same parameters are set out in Table 3.

530  The MF-gel exhibited a mean particle aggregate size of 141 ± 3 nm, slightly larger

531  than the mean particle aggregate size in UF-gel, 135 ± 8 nm. Concerning the rennet-induced

532  gels, it is known that in milk that has been heated, the κ-casein is broken down by chymosin

533  (as it is in unheated milk), but that the micelles do not aggregate well (Kethireddipalli, Hill, &

534  Dalgleish, 2011). This is due to the presence of denatured whey proteins on the micellar

535  surface, which may hinder the close approach of the potentially interacting sites on the

536  micelles (Dalgleish & Corredig, 2012). Waungana, Singh, & Bennett (1996) observed that the

537  denaturation of individual whey proteins and their association with the casein micelles

538  resulted in prolonged gelation times and reduced gel firmness in gels produced from heat-

539  treated UF milk (UHT system; 80°C to 140°C for 4s) due to the formation of a limited

540  number of reactive sites at the micellar surface. It may thus follow that the denatured whey

541  proteins associated on the micellar surface in the UF concentrate prevented the close approach

542    of casein micelles, resulting in smaller particle aggregates in the (heat-treated) UF-gel when

543    compared with the MF-gel.

544        As expected, the mean particle aggregate size is larger in the two gels studied

545    compared with the mean particle size in the corresponding suspensions. This may be

546    explained by the aggregation of casein micelles in gels as a consequence of the addition of the

547    coagulant agent (rennet) (Walstra, Bloomfield, Jason Wei, & Jenness, 1981).

548        Mean inter-particle aggregate distances were shown by image analysis as $147 \pm 5$ nm

549    for the MF-gel, significantly greater than the mean value of $131 \pm 7$ nm obtained for the UF-

550    gel. The MF-gel contained particle aggregates and inter-particle aggregate distances greater

551    than those found in the UF-gel. These results are consistent with the boundary length unit area

552    values obtained for these gels.

553        The boundary length per unit area for the UF-gel was $10.7 \pm 0.7$ μm/μm$^2$, significantly

554    larger ($p < 0.05$) than the value found for the MF-gel, $9.5 \pm 0.3$ μm/μm$^2$. The boundary length

555    per unit area values obtained for the gels were larger when the particle aggregate sizes were

556    smaller (Table 3). This result was expected because matrices with smaller particle aggregates

557    present more interfaces (particle aggregates/aqueous phase).

558        Values of boundary length per unit area were significantly larger ($p < 0.05$) in the gels

559    when compared to suspensions. This result was also expected because particle sizes in

560    suspensions were found to be significantly smaller ($p < 0.05$) than particle aggregate sizes in

561    gels. Therefore, in suspensions, more interfaces (particle/aqueous phase) were present,

562    resulting in bigger values of boundary length per unit area values.

563        Tortuosity values were similar for the two concentrated milk gels ($1.5 \pm 0.2$ and $1.5 \pm$

564    $0.2$ for MF- and UF-gels, respectively). These values are much larger than for the

565    suspensions. This corresponds to the increase in the aggregate size, which leads to longer

23

566  paths between given points. In this study, the tortuosity value could not enable discrimination

567  between different gel microstructures but with similar casein composition.

568

569  **4. Conclusions**

570

571       An automated image analysis procedure for microstructural characterization of dairy

572  systems was developed. The procedure was first applied to models of synthetic suspensions,

573  and then on milk suspensions (with comparison with published data) to validate the

574  methodology. The computerized image analysis method enabled an easy measurement of a

575  series of microstructural parameters of milk gels, which makes it especially useful for routine

576  measurements.

577       The measurements of the area fraction (and hence of the sample porosity) were similar

578  for the MF- and UF-suspensions, and for the MF- and UF-gels. The image analysis procedure

579  made it possible to quantify differences of microstructure independently of the area fraction.

580  Binary image granulometry measures particle size distribution that can also be represented by

581  an average particle size. In a similar way, the distribution of distances between particles can

582  be represented by an average value. These two measurements can describe dairy systems by

583  using parameters that can be easily interpreted and compared.

584       The measurement of boundary length per unit area indicates the complexity of the

585  matrix microstructure, without making the assumption that the system is a collection of

586  particles. In case of particles systems with a similar area fraction, this parameter seems to be

587  correlated with the average particle size.

588       The tortuosity of a sample describes the complexity of the aqueous phase, and is

589  expected to be related to diffusion properties. In this study, the measured values were

590  different for suspensions and gels, but no difference could be discerned between the two gels

591 studied (obtained with different preparation methods). Tortuosity is difficult to measure when

592 the area fraction of the solid phase is large: when the aggregates are large, the probability of

593 observing non-connected aqueous phases increases. An alternative could be to allow the

594 computation of geodesic distances in both phases but using different propagation speeds (Wu

595 et al., 2006), or to consider the tortuosity over a limited distance.

596 It was demonstrated that the image analysis method for the estimation of

597 microstructural parameters was able to differentiate between dairy systems of similar

598 composition, but obtained from different processes.

599 For a better understanding of the microstructure of dairy systems, modeling

600 approaches might be considered. In this study, we have simulated binary images similar to

601 suspension images, with the objective of validating the image analysis methodology.

602 However, the microstructure of milk gels is much more complex and involves a variety of

603 physical and chemical processes. Several modeling approaches have already been undertaken

604 by other authors to reconstruct the microstructure based on 2D or 3D observations (Yeong &

605 Torquato, 1998; Kumar, Briant, & Curtin, 2006; Nisslert, Kvarnström, Loren, Nyden, &

606 Rudemo, 2007; Jiang, Chen, & Burkhart, 2013). Similar approaches could be investigated for

607 dairy systems.

608 The developed image analysis procedure enables new insights into the characterization

609 of the microstructure of dairy systems. This approach, which was applied to milk gels, might

610 be adapted and extended to other food systems.

611 This procedure can also contribute to a better understanding of the effects of

612 processing on the structure-property relationships in dairy products. For instance, further work

613 might focus on coupling measurements obtained by image analysis, which describe the

614 microstructure of milk gels, to physical phenomena such as diffusion properties.

615

616 **Acknowledgments**

617

**References**

624

625    Aguilera, J. M., Stanley, D. W., & Baker, K. M. (2000). New dimensions in microstructure of
626        food products. *Trends in Food Science & Technology, 11*(1), 3-9.

627    Aly, S., Floury, J., Famelart, M. H., Madec, M. N., Dupont, D., Le Gouar, Y. et al. (2011).
628        Nisin quantification by ELISA allows the modeling of its apparent diffusion
629        coefficient in model cheeses. *Journal of Agricultural and Food Chemistry, 59*(17),
630        9484-9490.

631    Andrey, P. & Maurin, Y. (2005). Free-D: an integrated environment for three-dimensional
632        reconstruction from serial sections. *Journal of Neuroscience Methods, 145*(1–2), 233-
633        244.

634    Anema, S. G. & Li, Y. (2003). Association of denatured whey proteins with casein micelles in
635        heated reconstituted skim milk and its effect on casein micelle size. *Journal of Dairy
636        Research, 70*, 73-83.

637    Bouchoux, A., Debbou, B., Gésan-Guiziou, G., Famelart, M.-H., & Doublier, J.-L. (2009).
638        Rheology and phase behavior of dense casein micelle dispersions. *The Journal of
639        Chemical Physics, 131*(16).

640    Büchheim, W. (1982). Aspects of sample preparation for freeze-fracture/freeze-etch studies of
641        proteins and lipids in food systems: a review. *Food Microstructure, 1*(2), 189-208.

642    Crossley, J. I. & Aguilera, J. M. (2001). Modeling the effect of microstructure on food
643        extraction. *Journal of Food Process Engineering, 24*(3), 161-177.

644    Dalgleish, D. G. & Corredig, M. (2012). The structure of the casein micelle of milk and its
645        changes during processing. *Annual Review of Food Science and Technology, 3*(1),
646        449-467.

647    Delarue, A. & Jeulin, D. (2003). 3D morphological characterization of composite materials
648        with spherical aggregates. *Image Analysis and Stereology, 22*, 153-161.

649    El-Bakry, M. & Sheehan, J. (2014). Analysing cheese microstructure: A review of recent
650        developments. *Journal of Food Engineering, 125*, 84-96.

651 Ercili-Cura, D., Lille, M., Legland, D., Gaucel, S., Poutanen, K., Partanen, R. et al. (2013).
652    Structural mechanisms leading to improved water retention in acid milk gels by use of
653    transglutaminase. *Food Hydrocolloids, 30*(1), 419-427.

654 Fallico, V., Tuminello, L., Pediliggieri, C., Horne, J., Carpino, S., & Licitra, G. (2006).
655    Proteolysis and microstructure of Piacentinu Ennese cheese made using different farm
656    technologies. *Journal of Dairy Science, 89*(1), 37-48.

657 Fenoul, F., Le Denmat, M., Hamdi, F., Cuvelier, G., & Michon, C. (2008). Technical Note:
658    Confocal Scanning Laser Microscopy and quantitative image analysis: Application to
659    cream cheese microstructure investigation. *Journal of Dairy Science, 91*(4), 1325-
660    1333.

661 Fox, P. F. & Brodkorb, A. (2008). The casein micelle: Historical aspects, current concepts and
662    significance. *International Dairy Journal, 18*(7), 677-684.

663 Fucà, N., Pasta, C., Impoco, G., Caccamo, M., & Licitra, G. (2013). Microstructural
664    properties of milk fat globules. *International Dairy Journal, 31*(1), 44-50.

665 Geng, X. L., van den Berg, F. W. J., Bager, A. N., & Ipsen, R. (2011). Dynamic visualization
666    and microstructure of syneresis of cheese curd during mechanical treatment.
667    *International Dairy Journal, 21*(9), 711-717.

668 Goff, H. D., Verespej, E., & Smith, A. K. (1999). A study of fat and air structures in ice
669    cream. *International Dairy Journal, 9*(11), 817-829.

670 Gunasekaran, S. & Ding, K. (1999). Three-dimensional characteristics of fat globules in
671    cheddar cheese. *Journal of Dairy Science, 82*(9), 1890-1896.

672 Hussain, I., Grandison, A. S., & Bell, A. E. (2012). Effects of gelation temperature on
673    Mozzarella-type curd made from buffalo and cows milk. 1: Rheology and
674    microstructure. *Food Chemistry, 134*(3), 1500-1508.

675 Impoco, G., Carrato, S., Caccamo, M., & Tuminello, L. (2006). Quantitative analysis of
676    cheese microstructure using SEM imagery. In *SIMAI 2006 Minisymposium: Image
677    Analysis Methods for Industrial Application*.

678 Impoco, G., Fucà, N., Pasta, C., Caccamo, M., & Licitra, G. (2012). Quantitative analysis of
679      nanostructures shape and distribution in micrographs using image analysis. *Computers*
680      *and Electronics in Agriculture, 84*, 26-35.

681 Jeurnink, T. J. M. & de Kruif, K. G. (1993). Changes in milk on heating: viscosity
682      measurements. *Journal of Dairy Research, 60*(2), 139-150.

683 Jiang, G. Z., Chen, W., & Burkhart, C. (2013). Efficient 3D porous microstructure
684      reconstruction via Gaussian random field and hybrid optimization. *Journal of*
685      *Microscopy, 252*(2), 135-148.

686 Kalab, M., Allan-Wojtas, P., & Mistry, V. V. (1995). Microscopy and other imaging
687      techniques in food structure analysis. *Trends in Food Science & Technology, 6*, 3210-
688      3218.

689 Karlsson, A. O., Ipsen, R., Schrader, K., & Ardö, Y. (2005). Relationship between physical
690      properties of casein micelles and rheology of skim milk concentrate. *Journal of Dairy*
691      *Science, 88*(11), 3784-3797.

692 Kethireddipalli, P., Hill, A. R., & Dalgleish, D. G. (2011). Interaction between casein micelles
693      and whey protein/kappa-casein complexes during renneting of heat-treated
694      reconstituted skim milk powder and casein micelle/serum mixtures. *Journal of*
695      *Agricultural and Food Chemistry, 59*(4), 1442-1448.

696 Kumar, H., Briant, C. L., & Curtin, W. A. (2006). Using microstructure reconstruction to
697      model mechanical behavior in complex microstructures. *Mechanics of Materials,*
698      *38*(8−10), 818-832.

699 Lanfrey, P. Y., Kuzeljevic, Z. V., & Dudukovic, M. P. (2010). Tortuosity model for fixed
700      beds randomly packed with identical particles. *Chemical Engineering Science, 65*(5),
701      1891-1896.

702 Latour, L. L., Kleinberg, R. L., Mitra, P. P., & Sotak, C. H. (1995). Pore-size distributions and
703      tortuosity in heterogeneous porous media. *Journal of Magnetic Resonance, Series A,*
704      *112*(1), 83-91.

705 Le Feunteun, S. & Mariette, F. (2007). Impact of casein gel microstructure on self-diffusion
706        coefficient of molecular probes measured by $^1$H PFG-NMR. *Journal of Agricultural*
707        *and Food Chemistry, 55*(26), 10764-10772.

708 Le Feunteun, S. & Mariette, F. (2008). PFG–NMR techniques provide a new tool for
709        continuous investigation of the evolution of the casein gel microstructure after
710        renneting. *Macromolecules, 41*(6), 2071-2078.

711 Legland, D., Devaux, M. F., Bouchet, B., Guillon, F., & Lahaye, M. (2012). Cartography of
712        cell morphology in tomato pericarp at the fruit scale. *Journal of Microscopy, 247*(1),
713        78-93.

714 Legland, D., Kiêu, K., & Devaux, M. F. (2007). Computation of Minkowski measures on 2D
715        and 3D binary images. *Image Analysis and Stereology, 26*(6), 83-92.

716 Lucey, J. A. (2002). Formation and physical properties of milk protein gels. *Journal of Dairy*
717        *Science, 85*(2), 281-294.

718 Marchesseau, S., Gastaldi, E., Lagaude, A., & Cuq, J. L. (1997). Influence of pH on protein
719        interactions and microstructure of process cheese. *Journal of Dairy Science, 80*(8),
720        1483-1489.

721 Maubois, J. L. & Mocquot, G. (1971). Préparation de fromage à partir de "pré-fromage
722        liquide" obtenu par ultrafiltration du lait. *Lait, 51*(508), 495-533.

723 Maubois, J. L. & Mocquot, G. (1975). Application of membrane ultrafiltration to preparation
724        of various types of cheese. *Journal of Dairy Science, 58*(7), 1001-1007.

725 Maubois, J. L., Mocquot, G., & Vassal, L. (1969). A method for processing milk and milk
726        products. [2052121]. French.

727 McMahon, D. J., Fife, R. L., & Oberg, C. J. (1999). Water partitioning in Mozzarella cheese
728        and its relationship to cheese meltability. *Journal of Dairy Science, 82*(7), 1361-1369.

729 McMahon, D. J. & McManus, W. R. (1998). Rethinking casein micelle structure using
730        electron microscopy. *Journal of Dairy Science, 81*(11), 2985-2993.

731    Mellema, M., Heesakkers, J. W. M., van Opheusden, J. H. J., & van Vliet, T. (2000).
732        Structure and scaling behavior of aging rennet-induced casein gels examined by
733        confocal microscopy and permeametry. *Langmuir, 16*(17), 6847-6854.

734    Morand, M., Guyomarc'h, F., Legland, D., & Famelart, M. H. (2012). Changing the
735        isoelectric point of the heat-induced whey protein complexes affects the acid gelation
736        of skim milk. *International Dairy Journal, 23*(1), 9-17.

737    Nair, P. K., Dalgleish, D. G., & Corredig, M. (2013). Colloidal properties of concentrated
738        heated milk. *Soft Matter, 9*(14), 3815-3824.

739    Nisslert, R., Kvarnström, M., Loren, N., Nyden, M., & Rudemo, M. (2007). Identification of
740        the three-dimensional gel microstructure from transmission electron micrographs.
741        *Journal of Microscopy, 225*(1), 10-21.

742    Ohser, J. & Mücklich, F. (2000). *Statistical analysis of microstructures in materials sciences*.
743        (1th ed.). Chichester: John Wiley & Sons.

744    Ong, L., Dagastine, R. R., Kentish, S. E., & Gras, S. L. (2011). Microstructure of milk gel and
745        cheese curd observed using cryo scanning electron microscopy and confocal
746        microscopy. *Food Science and Technology, 44*(5), 1291-1302.

747    Ong, L., Dagastine, R. R., Kentish, S. E., & Gras, S. L. (2012). The effect of pH at renneting
748        on the microstructure, composition and texture of Cheddar cheese. *Food Research*
749        *International, 48*(1), 119-130.

750    Ong, L., Dagastine, R. R., Kentish, S. E., & Gras, S. L. (2013). The effect of calcium chloride
751        addition on the microstructure and composition of Cheddar cheese. *International*
752        *Dairy Journal, 33*(2), 135-141.

753    Otsu, N. (1979). A threshold selection method from gray-level histograms. *IEEE Transactions*
754        *on Systems, Man, and Cybernetics, 9*(1), 62-66.

755    Ramasubramanian, L., Webb, R., D'Arcy, B., & Deeth, H. C. (2013). Characteristics of a
756        calcium−milk coagulum. *Journal of Food Engineering, 114*(2), 147-152.

757    Reis, P. J. M. & Malcata, F. X. (2011). Ripening-related changes in Serra da Estrela cheese: A
758        stereological study. *Journal of Dairy Science, 94*(3), 1223-1238.

759    Rovira, S., Lopez, M. B., Ferrandini, E., & Laencina, J. (2011). Hot topic: Microstructure
760            quantification by scanning electron microscopy and image analysis of goat cheese
761            curd. *Journal of Dairy Science, 94*(3), 1091-1097.

762    Sam Saguy, I., Marabi, A., & Wallach, R. (2005). New approach to model rehydration of dry
763            food particulates utilizing principles of liquid transport in porous media. *Trends in*
764            *Food Science & Technology, 16*(11), 495-506.

765    Shen, L. & Chen, Z. (2007). Critical review of the impact of tortuosity on diffusion. *Chemical*
766            *Engineering Science, 62*(14), 3748-3755.

767    Silva, J. V. C., Peixoto, P. D. S., Lortal, S., & Floury, J. (2013). Transport phenomena in a
768            model cheese: The influence of the charge and shape of solutes on diffusion. *Journal*
769            *of Dairy Science, 96*(10), 6186-6198.

770    Singh, H. & Waungana, A. (2001). Influence of heat treatment of milk on cheesemaking
771            properties. *International Dairy Journal, 11*(4–7), 543-551.

772    Smith, A. K., Kakuda, Y., & Goff, H. D. (2000). Changes in protein and fat structure in
773            whipped cream caused by heat treatment and addition of stabilizer to the cream. *Food*
774            *Research International, 33*(8), 697-706.

775    Soille, P. (2003). *Morphological Image Analysis: Principles and Applications*. (2 ed.).
776            Secaucus, NJ, USA: Springer-Verlag New York, Inc.

777    Srilaorkul, S., Ozimek, L., Ooraikul, B., Hadziyev, D., & Wolfe, F. (1991). Effect of
778            ultrafiltration of skim milk on casein micelle size distribution in retentate. *Journal of*
779            *Dairy Science, 74*(1), 50-57.

780    Suman, R. & Ruth, D. (1993). Formation factor and tortuosity of homogeneous porous media.
781            *Transp Porous Med, 12*(2), 185-206.

782    Torquato, S. (2002). *Random heterogeneous materials: microstructure and macroscopic*
783            *properties*. New York: Springer-Verlag.

784    Ulve, V. M., Monnet, C., Valence, F., Fauquant, J., Falentin, H., & Lortal, S. (2008). RNA
785            extraction from cheese for analysis of in situ gene expression of Lactococcus lactis.
786            *Journal of Applied Microbiology, 105*(5), 1327-1333.

787 Walstra, P., Bloomfield, V. A., Jason Wei, G., & Jenness, R. (1981). Effect of chymosin
788     action on the hydrodynamic diameter of casein micelles. *Biochimica et Biophysica*
789     *Acta (BBA) - Protein Structure, 669*(2), 258-259.

790 Waninge, R., Kalda, E., Paulsson, M., Nylander, T., & Bergenstahl, B. (2004). Cryo-TEM of
791     isolated milk fat globule membrane structures in cream. *Physical Chemistry and*
792     *Chemical Physics, 6*, 1518-1523.

793 Waninge, R., Nylander, T., Paulsson, M., & Bergenstahl, B. (2003). Milk membrane lipid
794     vesicle structures studied with cryo-TEM. *Colloids and Surfaces B: Biointerfaces,*
795     *31*(1-4), 257-264.

796 Waungana, A., Singh, H., & Bennett, R. J. (1996). Influence of denaturation and aggregation
797     of beta-lactoglobulin on rennet coagulation properties of skim milk and ultrafiltered
798     milk. *Food Research International, 29*(8), 715-721.

799 Wium, H., Pedersen, P. S., & Qvist, K. B. (2003). Effect of coagulation conditions on the
800     microstructure and the large deformation properties of fat-free Feta cheese made from
801     ultrafiltered milk. *Food Hydrocolloids, 17*(3), 287-296.

802 Wu, Y. S., van Vliet, L. J., Frijlink, H. W., & van der Voort Maarschalk, K. (2006). The
803     determination of relative path length as a measure for tortuosity in compacts using
804     image analysis. *European Journal of Pharmaceutical Sciences, 28*(5), 433-440.

805 Yeong, C. L. Y. & Torquato, S. (1998). Reconstructing random media. *Physical Review e,*
806     *57*(1), 495-506.

807 Zalc, J. M., Reyes, S. C., & Iglesia, E. (2004). The effects of diffusion mechanism and void
808     structure on transport rates and tortuosity factors in complex porous structures.
809     *Chemical Engineering Science, 59*(14), 2947-2960.

**Table Captions**

**Table 1**

Composition of the MF and UF concentrates.

**Table 2**

Values of parameters characterizing the microstructure of two concentrated milk suspensions (MF- and UF-suspensions) obtained from image analysis on binary micrographs[1].

**Table 3**

Values of parameters characterizing the microstructure of two concentrated milk gels (MF- and UF-gels) obtained from image analysis on binary micrographs[1].

**Figure Captions**

**Fig. 1.** Schematic representation of the automated segmentation procedure. The original TEM micrograph (A) is divided by a background image (B) to obtain a normalized image (C). The protein network is enhanced using a black top-hat filter (D), and smoothed to remove acquisition noise (E). Gray level histogram of the image, showing two peaks corresponding to the dark and white phases (F). The application of the Otsu threshold results in a binary image showing the protein phase as black and the void (aqueous) phase as white (G).

**Fig. 2.** Generation of a synthetic suspension of micelles. (A) 3D representation of a sample of the system of spheres (red) together with the region corresponding to the thick section (blue). (B) Sample binary image obtained by the intersection of the thick section with the system of spheres, projected along the z direction.

**Fig. 3.** Schematic representation of the microstructural parameters determined for dairy systems (suspensions and gels) by the image morphological granulometry method.

**Fig. 4.** Graphical illustration of tortuosity through a given point in a synthetic binary structure, computed as the ratio of the shortest lengths to borders (dashed line) over the image width (black line).

**Fig. 5.** TEM micrographs of concentrated milk suspensions and gels at 20000x magnification. (A) MF-suspension; (B) UF-suspension; (C) MF-gel; (D) UF-gel.

**Fig. 6.** Representative segmented TEM micrographs (binarised images) of concentrated milk suspensions and the related gels. (A) MF-suspension; (B) UF-suspension; (C) MF-gel; (D) UF-gel. These binarised images correspond to the TEM micrographs showed in Fig. 4.

**Fig. 7.** Distribution of particle sizes in TEM micrographs of (A) MF-suspension and (B) UF-suspension; Distribution of inter-particle distances in TEM micrographs of (C) MF-suspension and (D) UF-suspension.

**Fig. 8.** Distribution of particle aggregate sizes in TEM micrographs of (A) MF-gel and (B) UF-gel; Distribution of inter-particle aggregate distances in TEM micrographs of (C) MF-gel and (D) UF-gel.

| Product | Dry matter (g/kg) | Caseins (g/kg) | Whey proteins (g/kg) | Lactose and Minerals (g/kg) | Other (g/kg) |
|---|---|---|---|---|---|
| MF concentrate | 196 | 130.3 | 4.4 | 60.1 | 1.6 |
| UF concentrate | 223 | 130.7 | 27.3 | 63.1 | 1.8 |

| Parameter | MF-suspension | UF-suspension |
|---|---|---|
| Area fraction | $0.34 \pm 0.02$ | $0.33 \pm 0.01$ |
| Porosity | $0.66 \pm 0.02$ | $0.67 \pm 0.01$ |
| Boundary length per unit area ($\mu m/\mu m^2$) | $13.3 \pm 0.5$ | $12.1 \pm 0.2^*$ |
| Particle size (nm) | $88 \pm 3$ | $99 \pm 4^*$ |
| Inter-particle distance (nm) | $123 \pm 5$ | $132 \pm 2^*$ |
| Tortuosity | $1.08 \pm 0.01$ | $1.06 \pm 0.01$ |

[1]The results are expressed as the mean ± standard deviation of the mean (n = 10).
* The means within a single row are significantly different ($p < 0.05$).

| Parameter | MF-gel | UF-gel |
|---|---|---|
| Area fraction | 0.49 ± 0.03 | 0.50 ± 0.02 |
| Porosity | 0.51 ± 0.03 | 0.50 ± 0.02 |
| Boundary length per unit area ($\mu m/\mu m^2$) | 9.5 ± 0.3 | 10.7 ± 0.7[*] |
| Particle aggregate size (nm) | 141 ± 3 | 135 ± 8[*] |
| Inter-particle aggregate distance (nm) | 147 ± 5 | 131 ± 7[*] |
| Tortuosity | 1.5 ± 0.2 | 1.5 ± 0.2 |

[1]The results are expressed as the mean ± standard deviation of the mean (n = 10).
[*] The means within a single row are significantly different ($p < 0.05$).

| Parameter | MF-gel | UF-gel |
|---|---|---|
| Area fraction | 0.49 ± 0.03 | 0.50 ± 0.02 |

A

B

A

B

C

D
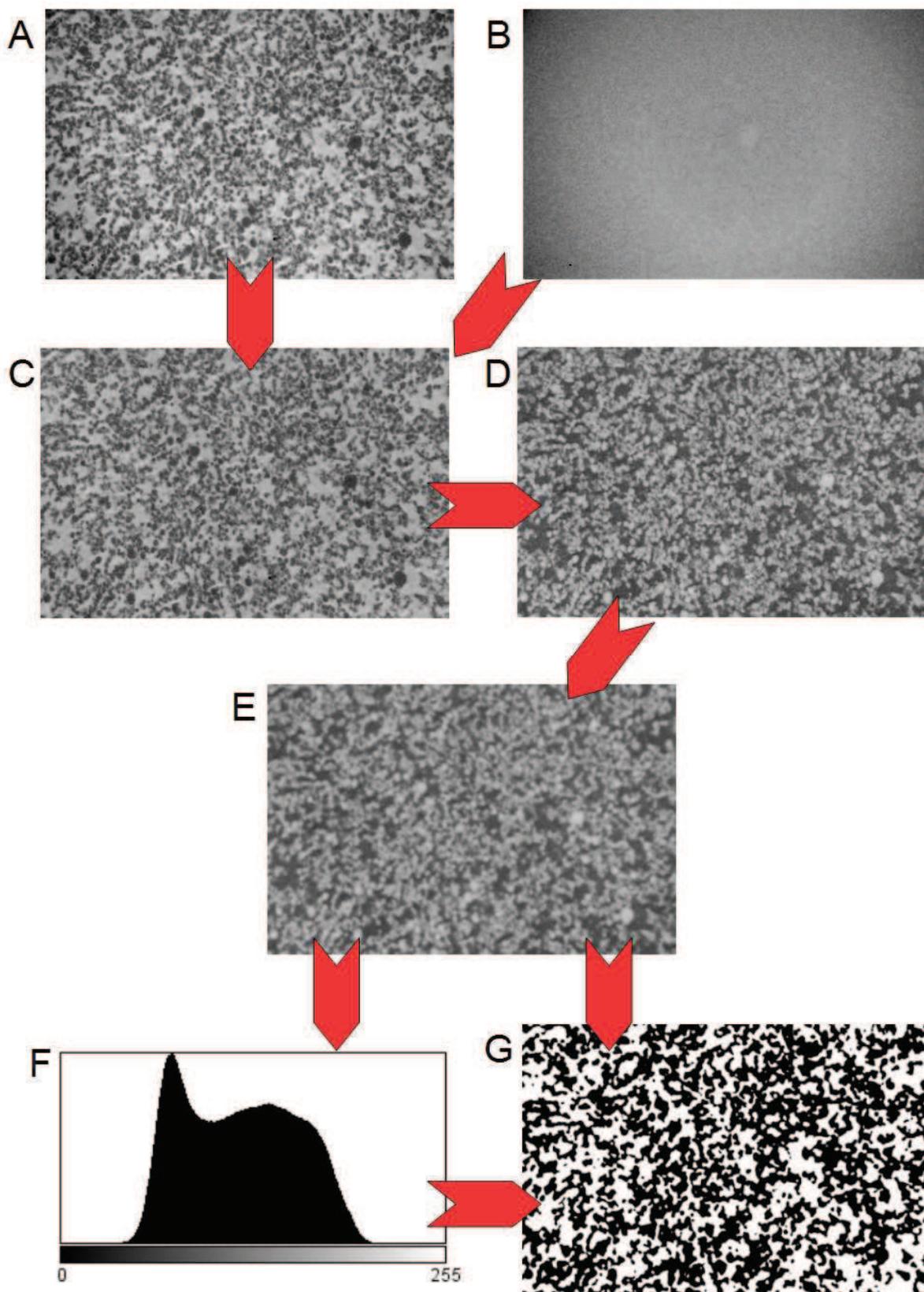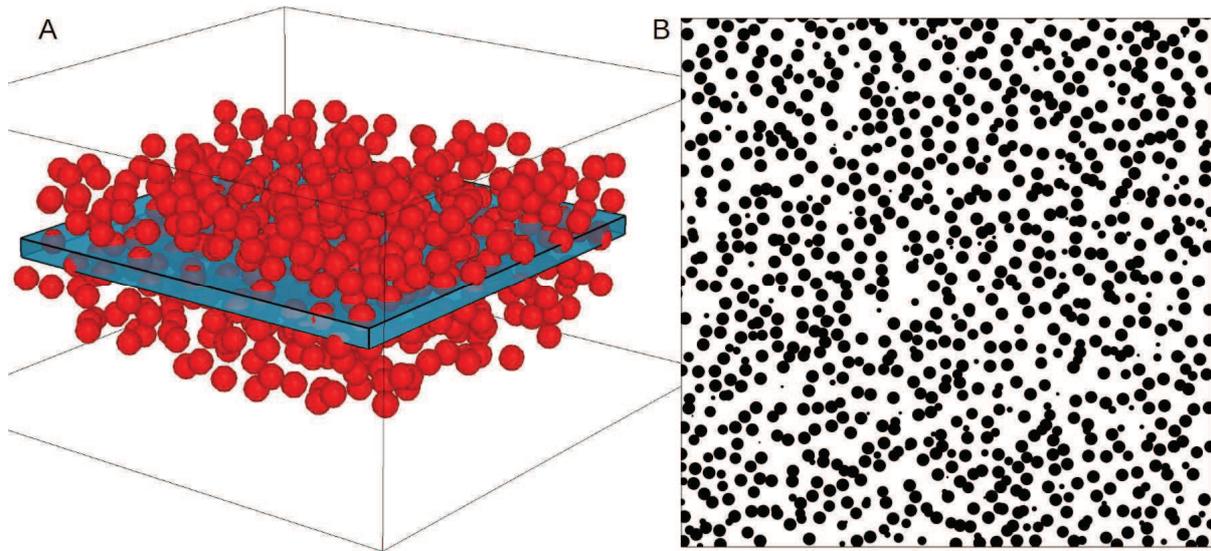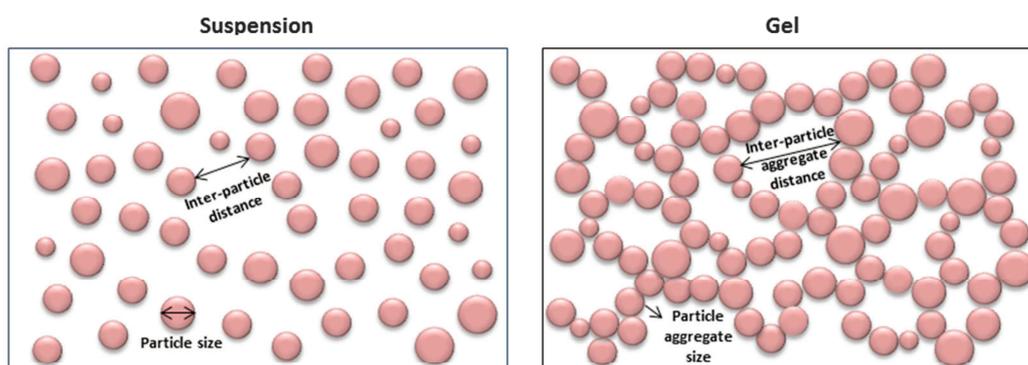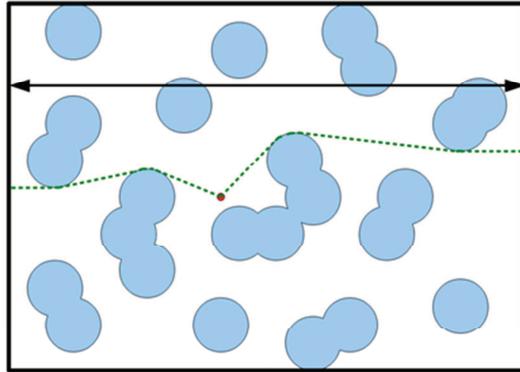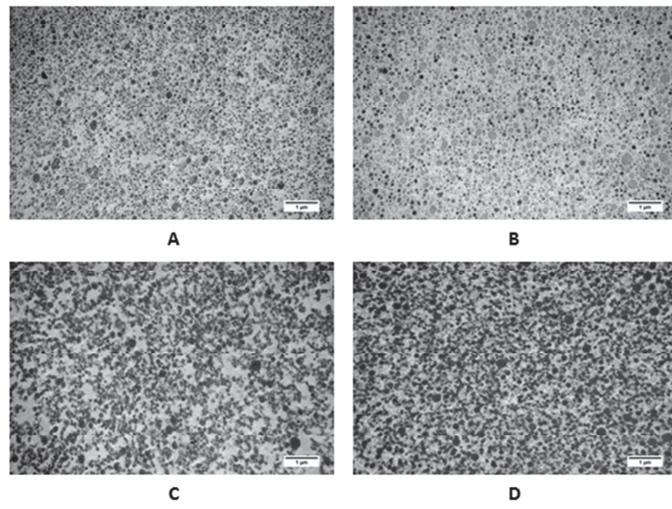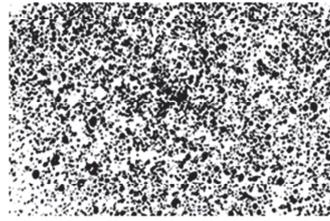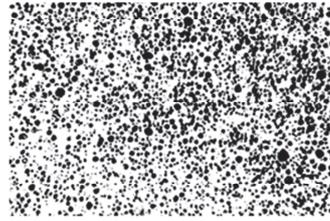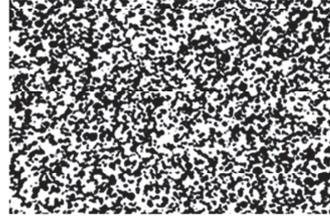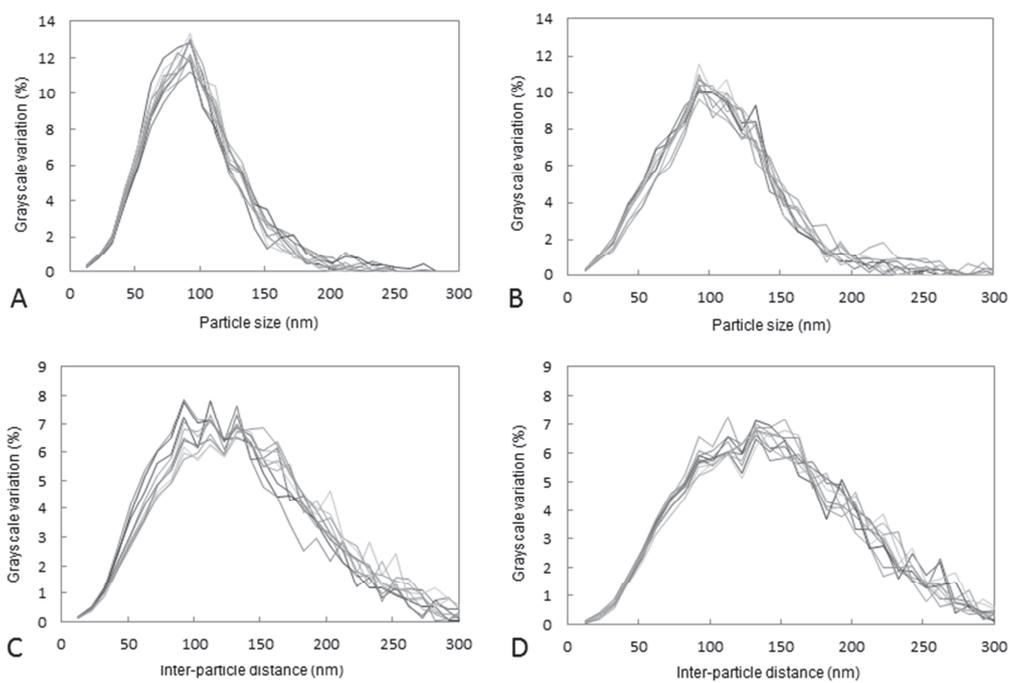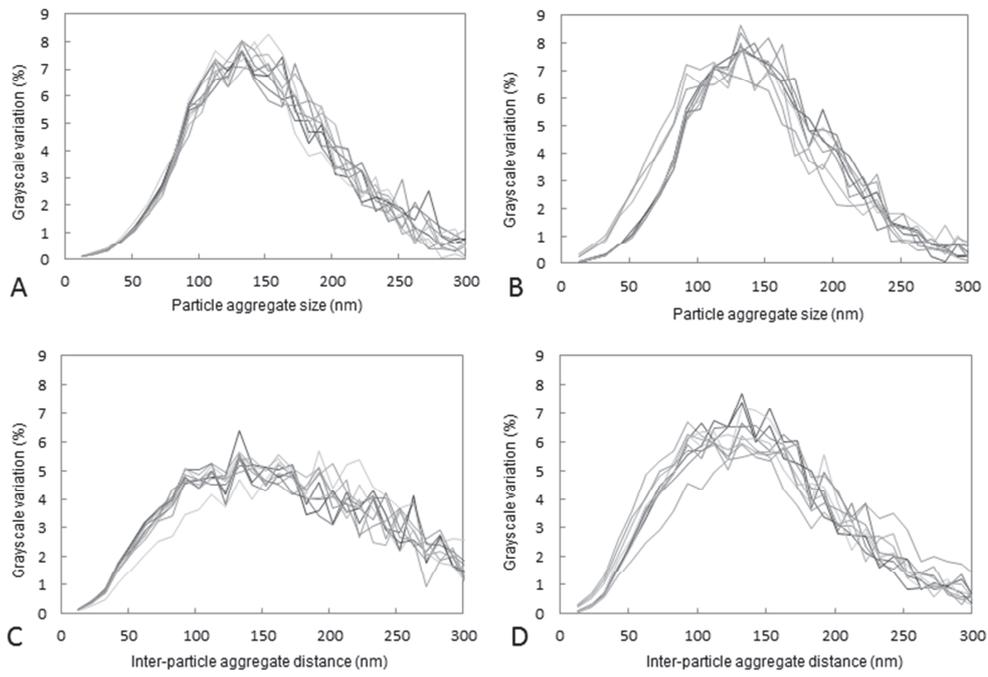
**Highlights**

- We developed a method of characterization of the microstructure of dairy systems.

- Microstructural parameters were determined by an automated image analysis method.

- These routine measurements provided discrimination between different dairy systems.

- This method applied to milk gels can be easily transferred to other food systems.